Macromolecular Research, Vol. 11, No. 1, pp 2-8 (2003)

Feature Article

Preparation of Polymeric Self-Assembly and Its Application to Biomaterials

Chong-Su Cho* and In-Kyu Park

School of Agricultural Biotechnology, Seoul National University, Suwon 441-744, Korea

Jae-Woon Nah

Department of Polymer Science and Engineering, Sunchon National University, Sunchon 540-742, Korea

Toshihiro Akaike

Department of Biomolecular Engineering, Tokyo Institute of Technology, Yokohama 226-8501, Japan

Received Aug. 19, 2002; Revised Jan. 28, 2003

Abstract: The self-assembly of polymers can lead to supramolecular systems and is related to the their functions of material and life sciences. In this article, self-assembly of Langmuir-Blodgett (LB) films, polymer micelles, and polymeric nanoparticles, and their biomedical applications are described. LB surfaces with a well-ordered and layered structure adhered more cells including platelet, hepatocyte, and fibroblast than the cast surfaces with microphase-separated domains. Extensive morphologic changes were observed in LB surface-adhered cells compared to the cast films. Amphiphilic block copolymers, consisting of poly(γ-benzyl L-glutamate) (PBLG) as the hydrophobic part and poly(ethylene oxide) (PEO) [or poly(*N*-isopropylacrylamide) (PNIPAAm)] as the hydrophilic one, can self-assemble in water to form nanoparticles presumed to be composed of the hydrophilic shell and hydrophobic core. The release characteristics of hydrophobic drugs from these polymeric nanoparticles were dependent on the drug loading contents and chain length of the hydrophobic part of the copolymers. Achiral hydrophobic merocyanine dyes (MDs) were self-assembled in copolymeric nanoparticles, which provided a chiral microenvironment as red-shifted aggregates, and the circular dichroism (CD) of MD was induced in the self-assembled copolymeric nanoparticles.

Keywords: self-assembly, Langmuir-Blodgett films, polymeric micelle, polymeric nanoparticles, induced circular dichroism.

Introduction

Self-assembly is a spontaneous association of molecules under equilibrium conditions into stable, structurally well-defined aggregates by noncovalent bonds,[1] eventually leading to the formation of supramolecular systems and taking responsibility over their functions. In material science, the concept of function through self-assembly contributed to the development of new materials. Furthermore, through studies on life sciences, we know that the biological functions such as stabilization of biomembranes, specific surface recognition, signal transduction, and information storage are closely related to the self-organization of biomolecules.[2] The self-assembled structures range from simple nematic liquid crystals, liposomes, micelles, and Langmuir-Blodgett (LB) films to complex biomembranes. This paper reviews LB films, polymeric micelles, and polymeric nanoparticles as polymeric self-assembly, and their applications in the biomedical fields.

*e-mail : chocs@plaza.snu.ac.kr

LB Films

Characteristics of LB Films. LB technique has been an attractive tool for arranging various molecules into well-defined ordered forms to develop ultrathin films for electronic and photoelectronic devices.[3,4] Typically, a monolayer is formed at the air/water interface, which is then converted into a condensed phase by compression,[5] and can be transferred by dipping and raising the substrate through the air/water interface. LB films have layered structures with a well-defined order or orientation of the functional moieties. In particular, monolayers of synthetic polypeptides as models for protein may be prepared, in which the polypeptide is in either the α-helical or β-sheet conformation, depending on the spreading solvent employed.[6] The chemical structure

schematic of a poly(γ-benzyl L-glutamate) (PBLG) family used by our group is shown in Figure 1.[7] Circular dichroism (CD) spectra of cast and LB films are shown in Figures 2 and 3, respectively. The spectrum of LB film is different from that of the cast film in that the former changed radically both in shape and in magnitude in response to the rotation of the sample. The angular dependence can be attributed to the orientation of PBLG film obtained by LB technique.[8] Polarized transmission FT-IR spectra of PBLG and block copolymer LB films revealed the main conformation of the molecules in the LB layer as well as in the cast film is α-helical, and the polypeptide α-helices are oriented with the main axis, parallel to the conformation direction for the LB films, in agreement with the CD data.[9]

Cell-LB Surface Interaction. In general, there are two types of cell interactions with the substratum. One is the non-specific interaction between cells and surfaces, such as ionic, hydrogen and hydrophobic bonds, and this type of attachment to the substratum is not mediated by extracellular matrix (ECM) proteins. The other involves specific interaction between adhesive ligands along the polymer chain and receptors on the cell surfaces. Unlike the former, this attachment is almost always mediated by ECM proteins.

Non-Specific Interaction between Cell and LB Surface: It is well-known that block or graft copolymer surfaces fabricated with microphase separated structure suppress the activation of adhering platelets, primarily due to the regulation and distribution of binding sites between platelets and the copolymer surface.[10] In an attempt to relate surface structure to the platelet adhesion of PBLG/poly(ethylene oxide) (PEO)/PBLG block copolymers (GEG), we compared the cellular behaviors between LB surface and the cast one, and found that much more platelets were adhered onto the block copolymer LB films than to the same block copolymer solvent cast onto surface.[11] The effect of PEO content on the LB film adhesion was antithetical. Furthermore, platelets adhered onto the PBLG/poly(propylene oxide) (PPO)/PBLG (GPG) cast film surface were round-shaped, whereas those adhered onto the LB film surface showed extended psuedopods and fried-egg appearances,[12] and this difference was found to be a similar tendency of platelets (Figure 4).[13] In most probability, PEO-based LB film surfaces may have been dominated by the hydrophobic PBLG component, and the PEO chains were restricted in their ability to migrate to the surface.[14]

Specific Interaction between Hepatocytes and LB Surface: Akaike *et al.* previously reported that poly(vinylbenzyl-β-D-lactonamide) (PVLA) is an artificial cellular matrix for the hepatocyte culture,[15] and that the adhesion is mediated by the galactose-specific interactions between hepatocyte and PVLA.[16] We studied the orientation effect of galactose ligand in PVLA on hepatocyte attachment. Results of hepatocyte adhesion between PBLG (or GEG) and PVLA LB films after albumin pretreatment indicated that hepatocyte adhesion for the PBLG or GEG LB surfaces decreased after the albumin

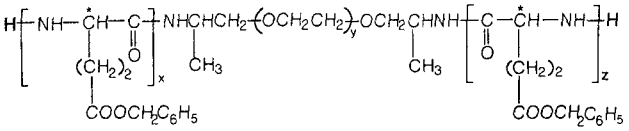

Figure 1. Chemical structure of PBLG/PEO/PBLG (GEG) block copolymer (from ref. 7).

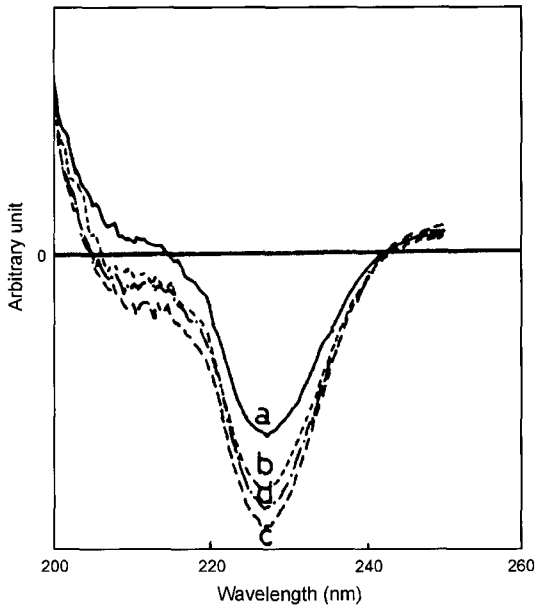

Figure 2. CD spectrum of cast film of PBLG according to the rotation: curve (a) 0°; curve (b) 90°; curve (c) 180°; curve (d) 270° (from ref. 8© Academic Press, Inc.).

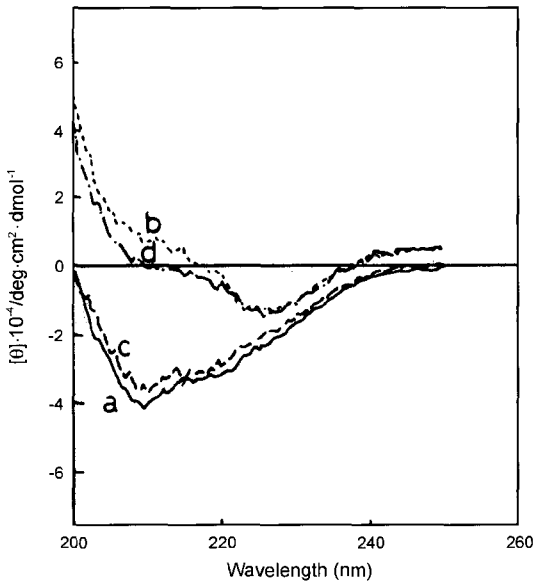

Figure 3. CD spectrum of LB film of PBLG according to the rotation: curve (a) 0°; curve (b) 90°; curve (c) 180°; curve (d) 270°; with 20 layers for the film (from ref. 8© Academic Press, Inc.).

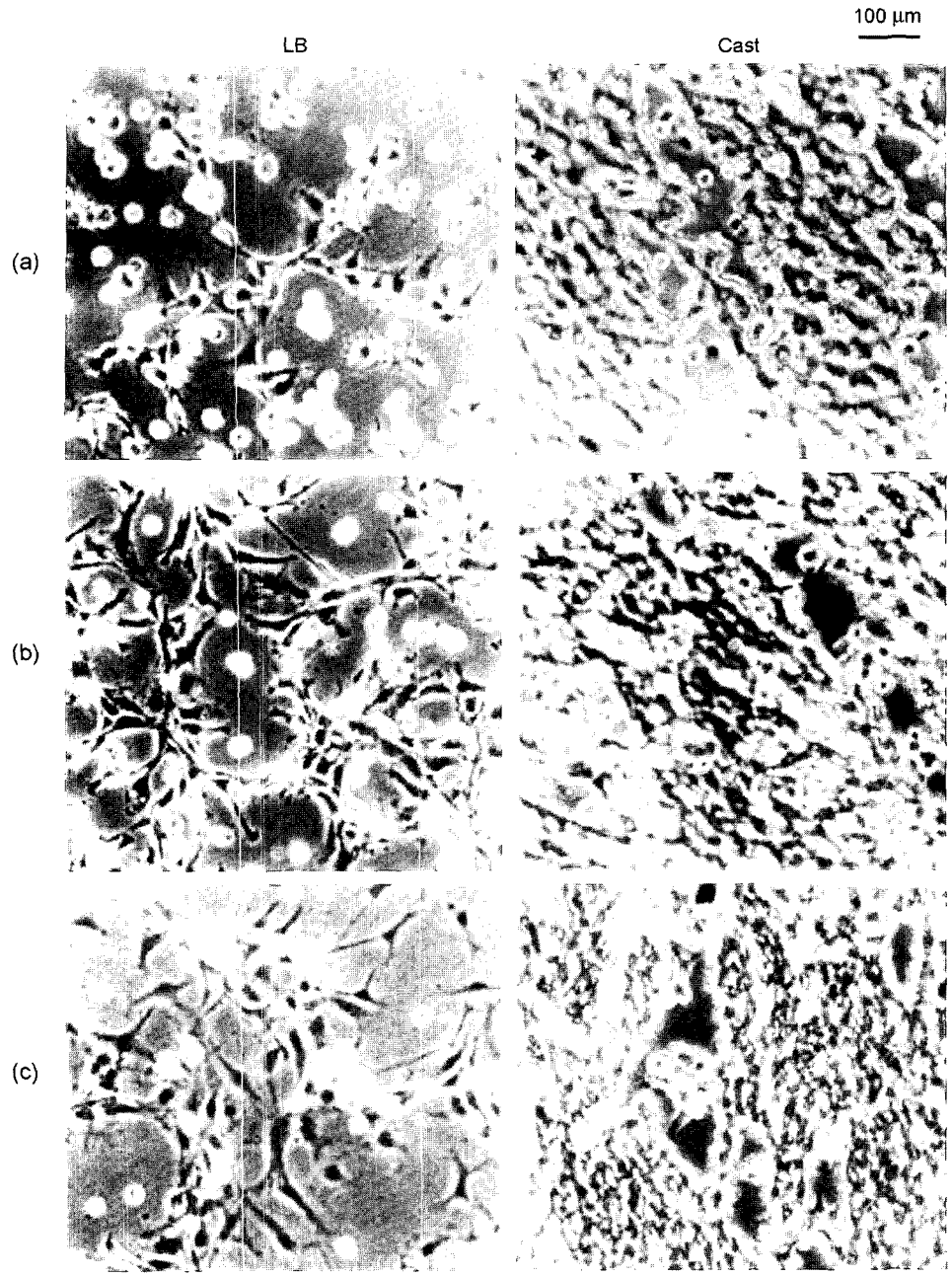

Figure 4. Phase-contrast microphotographs of fibroblast adherent onto the GE-3 (PEO: 39.0 mol%) copolymer: (a) 1 h, (b) 5 h, and (c) 23 h (from ref. 13 © John Wiley & Sons, Inc.).

treatment, whereas that for the PVLA LB one scarcely changed,[17] probably due to the albumin blocking of non-specific hydrophobic interactions between cells and LB surfaces. On the other hand, asialoglycoprotein antibody hindered the cell adhesion of the PVLA LB films. These findings thus reveal that adhesion of hepatocytes to the oriented PVLA LB surface is mediated by asialoglycoprotein receptors. Moreover, L929 cells cultivated on the collagen LB surface showed much higher adherence and spreadability than those on cast surface due to the higher -helix content in the LB surface than the cast one.[18]

Polymer Micelle

The assembly of polymers is mostly attained through the solvophobic interaction of solvent-insoluble blocks, whereas solvent-compatible blocks are selectively solvated by the solvents. The spherical micellar aggregates of amphiphilic

macromolecules in water have been investigated to clarify their micellar properties such as critical micelle concentration (CMC), size, shape, aggregation number, and structural stability, which depend on the conditions of the solution and the nature of the amphiphilic species such as chemical structure and solvophobicity of the amphiphile.[19,20] Polymeric micelles, with their numerous advantages including considerable thermodynamic stability, formation of hydrophobic core, small size, and hydrophilic outershell designed to minimize the potential for favorable interaction with other components of the environment such as physiological fluids or organs,[21,22] have attracted great attention for applications in drug delivery systems. The release behavior of the drug from the micelles is affected by the nature of the drug (solubility, crystallinity, etc.), the drug diffusion coefficient in the polymer, and the penetration of the release medium into the polymeric aggregates.

In our studies, the amphiphilic diblock copolymers comprising PBLG and polyether [or poly(*N*-isopropylacrylamide) (PNIPAAm)] as the hydrophobic and hydrophilic components, respectively, were synthesized by polymerization of γ-benzyl L-glutamate *N*-carboxyanhydride initiated by the primary amine located at the chain end of PEO (or PNIPAAm). The self-assembly with micellar structure of the above-mentioned block copolymers was obtained through diafiltration method

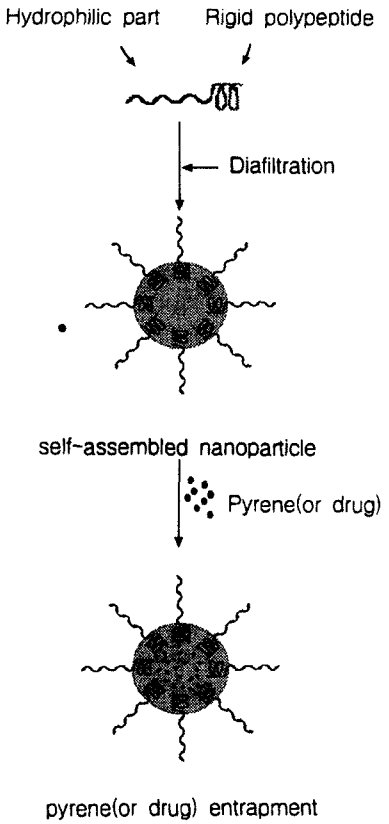

Scheme I. Physical entrapment of hydrophobic species (pyrene, drug) into the self-assembled nanoparticles (from ref. 23).

in water. During diafiltration, hydrophobic bonding was formed between the polypeptides possessing hydrophobic side-chain and rigid-rod backbone due to their α-helix comformation (the Scheme I).[23]

Shape of the PBLG/PEO block copolymer (GE) nanoparticles observed through SEM and TEM is spherical in general with size ranging about 50-200 nm (Figure 5).[24] The bright and dark images observed in the nanoparticles indicate that the self-assembly prepared from this block copolymer had two layers of core-shell nanoparticles. The dark part should be assigned to the hydrophobic core and the bright part to the hydrophilic shell. The particle size of GE-3 measured through dynamic light scattering (DLS) revealed a relatively large diameter compared to the result of TEM observation. The micelle sizes become larger as the content of PBLG in the block copolymer increases, because the micelle size increases until the free energy per molecule of micellization reaches the minimum level with increasing aggregation number.[25] The formation of the micelles for the polymers can be confirmed using the fluorescent probe method. The

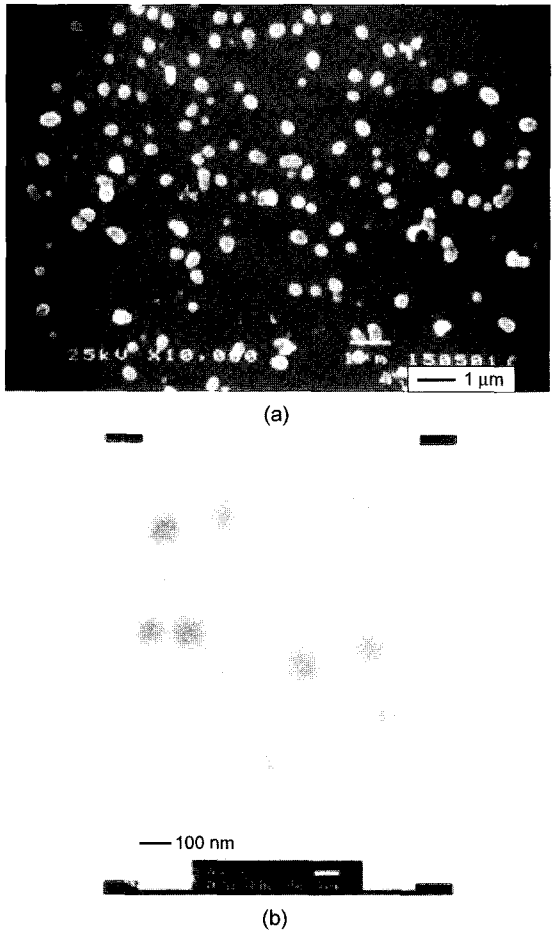

Figure 5. Scanning electron microscopy photograph (a) and transmission electron microscopy photograph (b) of GE-3 nanoparticles (from ref. 24 © Elsevier).

onset of intermolecular association of the amphiphilic block copolymers at the critical micelle concentration in water implies the formation of hydrophobic environment. At this point, a hydrophobic probe such as pyrene is preferentially solubilized into the inner part of this hydrophobic region of the aggregate. The transfer of pyrene from a polar environment to a nonpolar one leads to the changes in photophysical properties such as the increase in the quantum yield of the fluoresence, and a shift of the (0,0) band of the La($S_2 \leftarrow S_0$) transition from 333 to 339 nm. One can identify and determine CMC and equilibrium constant (K_v) for the partitioning of pyrene between the aqueous and the micelle core phases.[26] Figure 6(a) shows fluorescence excitation spectrum of pyrene in GE-2 aqueous solution at various polymer concentrations.[24]

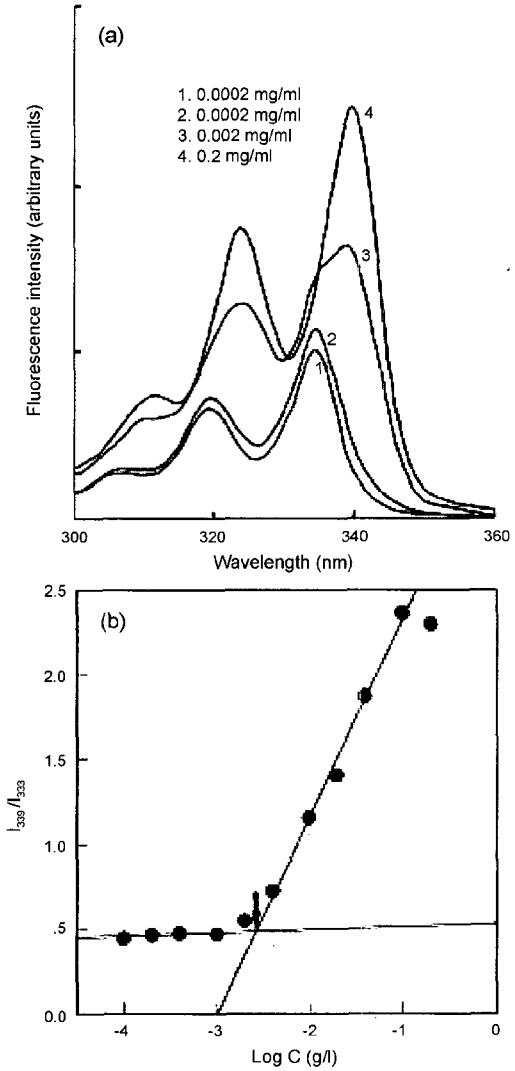

Figure 6. Fluorescence excitation spectrum of pyrene/GE-3 against concentration of GE-3 in distilled water (emission wavelength: 390.0 nm) (a) and plots of intensity ratio I_{339}/I_{333} from pyrene excitation spectrum vs. log c of the GE -3 copolymer in distilled water (b) (from ref. 24 © Elsevier).

The increase in the fluorescence intensity and the shift of the low-energy band from 334 to 339 nm were observed with increasing copolymer concentration. Dependence of I_{339}/I_{334} against the polymer concentration is taken as the intersection of two straight lines [Figure 6(b)]. The CMC values of the block copolymers decreased with increasing PBLG chain-length.

The release of drug from the PBLG/PNIPAAm nanoparticles, which exhibit interesting behavior due to the thermosensitivity of the shell, was studied *in vitro*,[27] and the results indicate that higher content of indomethacin (IN) from the nanoparticles was released at 28 °C than at 34 °C, because the expanded form of PNIPAAm in the shell part was changed into a compact one (Scheme II).

The nanoparticle sizes of hexablock copolymer (G_4E_2) based on PBLG and PEO as the hydrophobic and hydrophilic parts, respectively, range from 20 to 70 nm (Figure 7).[28]

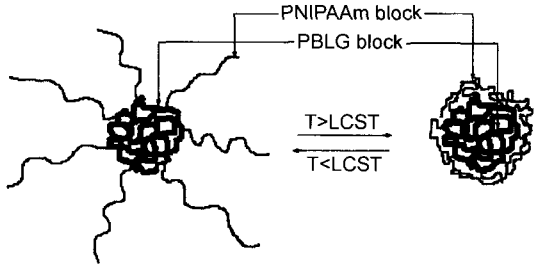

Scheme II. Schematic illustration of thermally-induced conformational changes for poly(γ-benzyl L-glutamate)/poly(*N*-isopropylacrylamide) (PBLG)/(PNIPAAm) (GN) core-shell type nanoparticle (LCST = lower critical solution temperature) (from ref. 27 © Hüthig & Wepf Verlag, Zug).

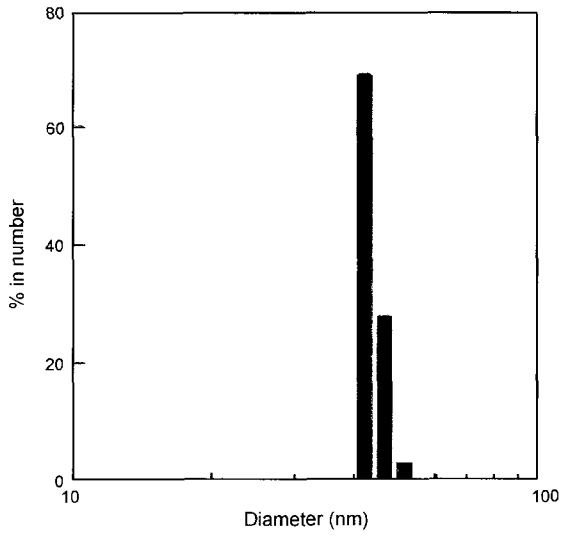

Figure 7. Particle size distribution of G_4E_2 by photon correlation spectroscopy. Concentration of G4E2 was 1.0 mg/mL measured at 25 °C (from ref. 30 © Elsevier).

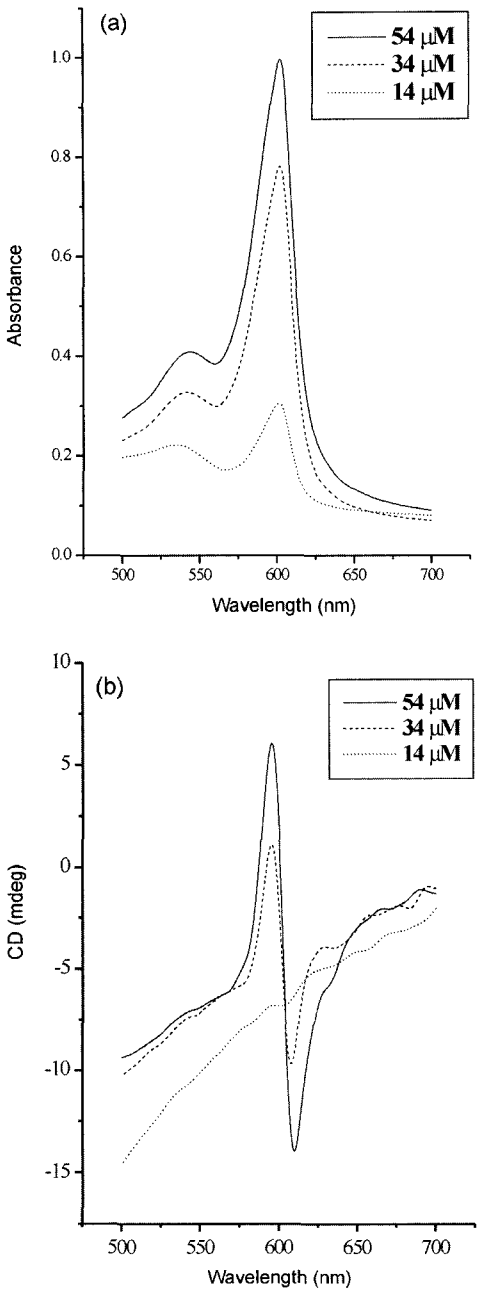

Figure 8. UV (a) and CD (b) spectra of MD loaded in the GE-3 nanoparticles in an MD concentration-dependent manner (from ref. 30 © Elsevier).

In addition, release of adriamycin (ADR) from the polymeric micelles *in vitro* was slower in longer PBLG chain-length and higher loading contents of ADR.[28]

Polymeric Nanoparticles

When the achiral compounds as guests were physically entrapped into the PBLG/PEO[29] or PBLG/PNIPAAm[30] nanoparticles as the host, they exhibited induced circular dichroism (ICD) caused by the chiral host. Figure 8 shows UV(a) and CD(b) spectra of the merocyanine dye (MD) in the GE-3 nanoparticles in a MD concentration-dependent manner. New absorption band appeared near 600 nm with a shoulder at around 540 nm. As reported previously, J-aggregates of MD appeared at 590 nm,[31] an indication that MDs existed as J-aggregate forms in the nanoparticles and the absorption peak of MD was red-shifted. In addition, J-aggregates of MD in the nanoparticles increased with increasing MD concentration. Two strong bands appeared in the CD spectrum [Figure 8(b)] at around J-aggregates of MD shown in the UV spectrum, an indication of ICD of MD by chiral PBLG in the PBLG/PEO block copolymer. The observed ICD spectrum of MD matched that of its UV absorption precisely. Thus, achiral MD exhibits Cotton effects through the chiral microenvironment of PBLG core in the self-assembled core-shell type nanoparticles and the interaction between the excited state of MDs under the chiral microenvironment gave an ICD curve with split Cotton effects on the basis of exciton coupling centered at 600 nm. Moreover, the Cotton effects of MD intensified with increasing concentration of MD in the GE-3 nanoparticles. These results together with the observed J-aggregate peak could suggest that MD molecules are aligned with a small slip angle (α).

Acknowledgements. The authors thank the Korea Science and Engineering Foundation (Grant No. 95-0300-10-3). This work was also supported by a grant provided by the Korean Ministry of Public Health and Welfare (02-PJ3-PG3-31402-0017).

References

(1) G. M. Whitesides, J. P. Mathias, and C. T. Seto, *Science*, **254**, 1312 (1991).
(2) H. Ringforf, B. Schlarb, and J. Venzmer, *Angew. Chem. Int. Ed. Engl.* **27**, 113 (1988).
(3) K. B. Blodgett, *J. Am. Chem. Soc.*, **57**, 1007 (1935).
(4) H. Kuhn, D. Mobius, and H. Bucher, *Techniques of Chemistry*, A. Weissberger and B. W. Rossiter, Eds., Wiley, New York, 1973, vol. 1, part 3B.
(5) C. S. Cho, R. Nagata, A. Yagawa, S. Takahashi, M. Kunou, and T. Akaike, *J. Polym. Sci., Part C : Polym. Lett.*, **28**, 89 (1990).
(6) D. W. Goupilk and F. C. Goodrich, *J. Colloid Interf. Sci.*, **62**, 142 (1977).
(7) C. S. Cho, S. W. Kim, and T. Komoto, *Makromol. Chem.*, **191**, 981 (1990).
(8) C. S. Cho, S. C. Song, M. Kunou, and T. Akaike, *J. Colloid Interf. Sci.*, **137**, 292 (1990).
(9) C. S. Cho, A. Kobayashi, M. Goto, and T. Akaike, *Thin Solid Films*, **264**, 82 (1995).
(10) T. Okano, K. Kataoka, Y. Sakurai, M. Shimada, T. Akaike,

and I. Shinohara, *Artificial Organs (Suppl.)*, **5**, 468 (1981).
(11) C. S. Cho, T. Takayama, M. Konou, and T. Akaike, *J. Biomed. Mat. Res.*, **24**, 1369 (1990).
(12) C. S. Cho, T. Kataoka, and T. Akaike, *J. Biomed. Mat. Res.*, **27**, 199 (1993).
(13) C. S. Cho, A. Kobayashi, M. Goto, K. H. Park, and T. Akaike, *J. Biomed. Mat. Res.*, **32**, 425 (1996).
(14) G. R. Llanos and M. V. Sefton, *J. Biomater. Sci. Polym. Ed.*, **4**, 381 (1993).
(15) A. Kobayashi, K. Kobayashi, and T. Akaike, *J. Biomater. Sci. Polym. Ed.*, **3**, 499 (1992).
(16) A. Kobayashi, M. Goto, K. Kobayashi, and T. Akaike, *J. Biomater. Sci. Polym. Ed.*, **6**, 325 (1994).
(17) C. S. Cho, M. Goto, A. Kobayashi, K. Kobayashi, and T. Akaike, *J. Biomater. Sci. Polym. Ed.*, **7**, 1097 (1996).
(18) A. Higuchi, S. Tamiya, T. Tsubomura, A. Katoh, C. S. Cho, T. Akaike, and M. Hara, *J. Biomater. Sci. Polym. Ed.*, **11**, 149 (2000).
(19) T. Kunitake, *Angew. Chem. Int. Ed. Engl.*, **31**, 709 (1992).
(20) X. F. Zhong, S. K. Varsheny, and A. Eisenberg, *Macromolecules*, **25**, 7160 (1992).
(21) D. Izzo and C. M. Marque, *Macromolecules*, **26**, 7189 (1993).
(22) K. Kataoka, G. S. Kwon, M. Yokohama, T. Okano, and Y. Sakurai, *J. Control. Release*, **24**, 119 (1993).
(23) J. B. Cheon, Y. I. Jeong, and C. S. Cho, *Korea Polym. J.*, **6**, 34 (1998).
(24) Y. I. Jeong, J. B. Cheon, S. H. Kim, J. W. Nah, Y. M. Lee, Y. K. Sung, T. Akaike, and C. S. Cho, *J. Control. Release*, **51**, 169 (1998).
(25) R. Nagarajan and K. Ganesh, *J. Phys. Chem.*, **90**, 5843 (1989).
(26) M. Wilhelm, C. L. Zhao, Y. Wang, R. Xu, M. A. Winnik, J. L. Mura, G. Riess, and M. D. Croucher, *Macromolecules*, **24**, 1033 (1991).
(27) C. S. Cho, J. B. Cheon, Y. I. Jeong, I. S. Kim, S. H. Kim, and T. Akaike, *Macromol. Rapid Commun.*, **18**, 361 (1997).
(28) Y. I. Jeong, J. W. Nah, H. C. Lee, S. H. Kim, and C. S. Cho, *Int. J. Pharma.*, **188**, 49 (1999).
(29) T. W. Chung, T. Akaike, Y. H. Park, and C. S. Cho, *Polymer*, **41**, 6415 (2000).
(30) T. W. Chung, B. J. Kim, S. Y. Park, T. Akaike, J. W. Nah, and C. S. Cho, *Macromolecules*, **33**, 8921 (2000).
(31) Y. Hirano, J. Kawata, Y. E. Miura, M. Sugi, and T. Ishii, *Thin Solid Films*, **327**, 345 (1998).